# When is polarimetric imaging preferable to intensity imaging for target detection?

François Goudail, J. Scott Tyo

# When is polarimetric imaging preferable to intensity imaging for target detection?

**François Goudail[1,*] and J. Scott Tyo[2]**

[1]*Laboratoire Charles Fabry de l'Institut d'Optique, CNRS, Universite Paris-Sud, Campus Polytechnique, RD 128, 91127 Palaiseau, France*
[2]*College of Optical Sciences, University of Arizona, Tucson, Arizona 85721, USA*
**Corresponding author: francois.goudail@institutoptique.fr*

Received October 18, 2010; accepted November 14, 2010;
posted November 23, 2010 (Doc. ID 136832); published December 23, 2010

We consider target detection in images perturbed with additive noise. We determine the conditions in which polarimetric imaging, which consists of analyzing of the polarization of the light scattered by the scene before forming the image, yields better performance than classical intensity imaging. These results give important information to assess the interest of polarimetric imaging in a given application. 

*OCIS codes:* 260.5430, 030.4280.

## 1. INTRODUCTION

Polarization images are measures of some characteristics of the polarization state of the light scattered by a scene. They can reveal contrast that does not appear in classical intensity images and find many applications in machine vision [1], remote sensing [2–4], biomedical imaging [5,6], and industrial control [7]. Active polarimetric imaging systems illuminate the scene with a controlled polarization state and analyze the polarization state of the light scattered by the scene. A lot of work has been done on the optimization of the illumination and analysis states for different signal processing tasks, such as estimation of the Stokes vector [8–12] or discrimination of targets from backgrounds [13–16]. However, these demonstrations of optimality usually assume that the illumination and analysis polarization states are purely polarized, and the problem remains to determine whether it is preferable to illuminate the scene with purely polarized or partially polarized light. A second open question is whether or not it is preferable to analyze the polarization state of the output light or simply measure its intensity. The answer to these questions depends on the type of information that is sought in the image. In this paper, we consider detection of a target of interest appearing against a background. In this case, the answer depends on the respective polarimetric characteristics of the target and of the background: the more they differ, the more polarimetric imaging is likely to be preferable to intensity imaging. However, it would be useful to have a quantitative way of answering this question, and this is the purpose of the present article.

In target detection applications, the relevant efficiency criterion is contrast (or discrimination ability) between a target and a background. Analysis of the contrast and its optimization in polarimetric images have been investigated in the radar [13,17] and in the optics [14–16,18] communities. It has been shown recently that, in the presence of additive Gaussian noise and when the illumination is purely polarized, the polarimetric imaging architecture that maximizes the contrast between a target and a background consists of acquiring a single intensity image with optimized illumination and analysis states [19]. In this paper, we precisely determine the conditions under which such an architecture performs better than simple intensity imaging in term of contrast, and we determine when it is preferable to use polarized illumination instead of unpolarized light. We show in particular that these conditions depend on whether the polarization of the light scattered by the scene is analyzed with a standard polarizer or acquired at the two outputs of a polarizing beam splitter. The results also depend on the origin of the additive noise that perturbs the measurements. In Section 2, we consider that the noise is only due to the sensor, whereas in Section 3, we assume that the dominant source of noise is shot noise due to passive light entering the imaging systems. We discuss and illustrate these results in Section 4, and give some conclusions and perspectives in Section 5.

## 2. OPTIMIZATION OF THE CONTRAST IN THE PRESENCE OF DETECTOR NOISE

We assume that the observed scene is composed of two regions: a target with Mueller matrix $M^a$ and a background with Mueller matrix $M^b$. We use the Mueller formalism to represent the polarimetric properties of the scene since we are interested in remote sensing or biomedical applications where scenes are often highly depolarizing and the Jones formalism [20] is inadequate. Our purpose is to determine the settings of the polarimetric imager for which this scene appears with the maximal contrast. In the next subsections, we will address this issue with two different types of imaging architecture that require one and two intensity measurements.

### A. Single Intensity Measurement

Let us consider the imaging setup represented in Fig. 1(a). The light source of intensity $I_0$ (expressed in number of photons) is assumed totally unpolarized. It passes through a polarization state generator (PSG) consisting of a homogeneous diattenuator whose two orthogonal eigenstates have the Stokes vectors $\mathbf{S}_{\|} = (1, \mathbf{s}^T)^T$ and $\mathbf{S}_{\perp} = (1, -\mathbf{s}^T)^T$, where $\mathbf{s}$ is a unit

 

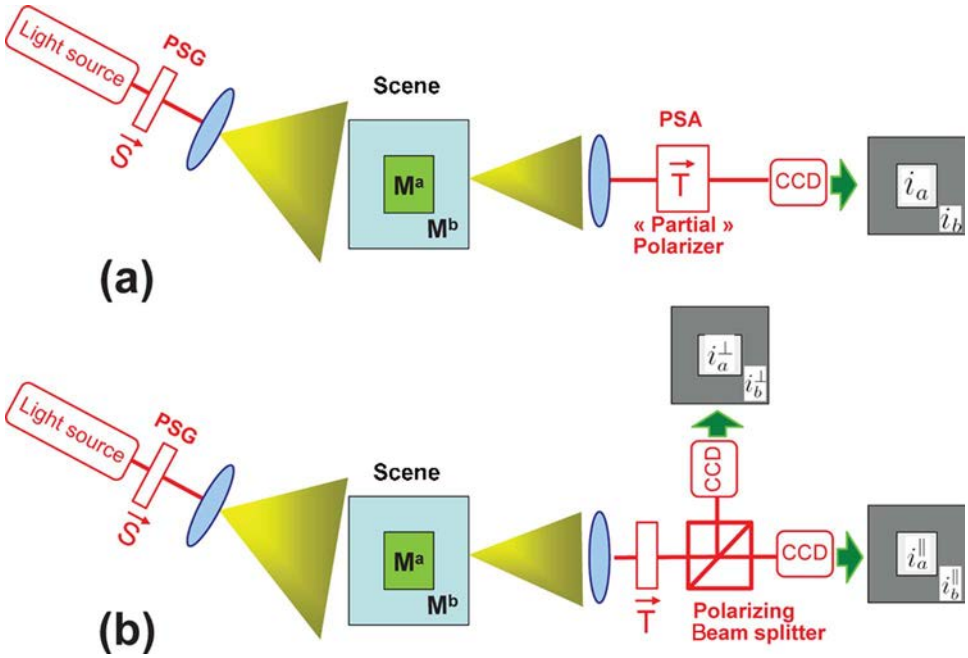


Fig. 1. (Color online) Polarimetric imaging setups. (a) Single intensity measurement. (b) Two intensity measurements.

norm, three-dimensional vector. The corresponding eigenvalues are $\lambda_\parallel$ and $\lambda_\perp$. We will assume, without loss of generality, that $\lambda_\parallel \geq \lambda_\perp$. This PSG model makes it possible to pass continuously from unpolarized illumination (when $\lambda_\parallel = \lambda_\perp$) to totally polarized illumination (when $\lambda_\perp = 0$). The illuminating light is scattered by the scene and analyzed by a polarization state analyzer (PSA) that also consists of a homogeneous diattenuator whose two orthogonal eigenstates are $\mathbf{T}_\parallel = (1, \mathbf{t}^T)^T$ and $\mathbf{T}_\perp = (1, -\mathbf{t}^T)^T$, where $\mathbf{t}$ is a unit norm, three-dimensional vector. The corresponding eigenvalues are $\mu_\parallel \geq \mu_\perp$. This PSA model makes it possible to pass continuously from standard intensity imaging (when $\mu_\parallel = \mu_\perp$) to polarimetric imaging with a perfect polarizer (when $\mu_\perp = 0$). This notation provides a way of defining precisely the notion of "partially polarized analyzer".

The light scattered by regions $a$ and $b$ is analyzed by the PSA, and the signal measured by the detector (expressed in number of photocounts per unit time) is

$$i_p = \frac{\eta}{4}[\mu_\parallel \mathbf{T}_\parallel + \mu_\perp \mathbf{T}_\perp]^T M^p [\lambda_\parallel \mathbf{S}_\parallel + \lambda_\perp \mathbf{S}_\perp] + n_p, \qquad (1)$$

where $p = \{a, b\}$, $\eta$ is the quantum efficiency of the detector, and $n_p$ is a zero mean Gaussian random variable with variance $\sigma^2$. We assume that this variance is independent of the parameters of the PSA. This is a pertinent model for noise that is generated by the detector itself, such as readout noise or dark current noise. It will thus be called in the following *detector noise*.

It is well known that the adequate expression of the contrast between a target and a background depends on the dominant source of noise that affects the image [21,22]. The additive Gaussian noise model leads to the following expression of the contrast [22]: $\mathcal{C}_D = (i_a - i_b)^2/\sigma^2$. Using Eq. (1), this contrast can also be written as

$$\mathcal{C}_D(\theta) = \frac{\lambda_\parallel^2 \mu_\parallel^2 \eta^2}{16\sigma^2} \times [(\mathbf{T}_\parallel + \beta \mathbf{T}_\perp)^T D (\mathbf{S}_\parallel + \alpha \mathbf{S}_\perp)]^2, \qquad (2)$$

where $\alpha = \lambda_\perp/\lambda_\parallel$, $\beta = \mu_\perp/\mu_\parallel$ (we notice that $\alpha$ and $\beta$ belong to $[0, 1]$); $\theta = (\mathbf{s}, \lambda_\parallel, \alpha, \mathbf{t}, \mu_\parallel, \beta)$ is the set of polarimetric parameters on which the contrast depends; and $D = M^a - M^b$. We will parametrize the matrix $D$ in the following way:

$$D = M^a - M^b = \begin{bmatrix} D_{00} & \mathbf{m}^T \\ \mathbf{n} & \tilde{D} \end{bmatrix}, \qquad (3)$$

where $D_{00}$ is a scalar, $\mathbf{m}$ and $\mathbf{n}$ are three-dimensional vectors, and $\tilde{D}$ is a $3 \times 3$ matrix. Note that $D$, being a difference of Mueller matrices, is not a Mueller matrix itself. Using this parametrization, the contrast in Eq. (2) can be written as

$$\begin{aligned}\mathcal{C}_D(\theta) = \frac{\lambda_\parallel^2 \mu_\parallel^2 \eta^2 I_0^2}{16\sigma^2} &[(1+\alpha)(1+\beta) D_{00} + (1-\alpha)(1+\beta)\mathbf{s}^T\mathbf{m} \\ &+ (1+\alpha)(1-\beta)\mathbf{t}^T\mathbf{n} + (1-\alpha)(1-\beta)\mathbf{t}^T\tilde{D}\mathbf{s}]^2. \end{aligned} \qquad (4)$$

Our objective is to determine the parameter set $\theta$ that maximizes the contrast. From Eq. (4), it is easily seen that, to maximize the contrast, $\lambda_\parallel$ and $\mu_\parallel$ must be as large as possible. For nonamplifying polarizers, $\lambda_\parallel, \mu_\parallel \leq 1$. We will thus set $\lambda_\parallel = \mu_\parallel = 1$ in the following. We also define the intensity signal-to-noise ratio

$$\mathrm{SNR}_D = \frac{\eta^2 I_0^2}{\sigma^2}, \qquad (5)$$

and $\theta' = (\mathbf{s}, \alpha, \mathbf{t}, \beta)$ is the set of parameters that remain to be optimized.

To investigate the influence of the parameter $\alpha$, we rewrite Eq. (4) as

$$\mathcal{C}_D(\theta') = \frac{\mathrm{SNR}_D}{16} \times [p + \alpha q]^2, \qquad (6)$$

with

$$\begin{aligned} p &= (1+\beta)(D_{00}+\mathbf{s}^T\mathbf{m})+(1-\beta)\mathbf{t}^T(\mathbf{n}+\tilde{D}\mathbf{s}) \\ q &= (1+\beta)(D_{00}-\mathbf{s}^T\mathbf{m})+(1-\beta)\mathbf{t}^T(\mathbf{n}-\tilde{D}\mathbf{s}). \end{aligned} \tag{7}$$

Since the function $f(\alpha)=[p+\alpha q]^2$ is convex, we have $\forall\alpha\in[0,1], f(\alpha)\le[f(0)+f(1)]/2\le\max[f(0),f(1)]$. Consequently, for any fixed values of $(\mathbf{s},\mathbf{t},\beta)$, including the optimal set, the contrast $\mathcal{C}_D(\theta')$ reaches its maximum for either $\alpha=0$ or $\alpha=1$.

To investigate the influence of the parameter $\beta$, we rewrite Eq. (4) as

$$\mathcal{C}_D(\theta')=\frac{\mathrm{SNR}_D}{16}\times[p'+\beta q']^2, \tag{8}$$

with

$$\begin{aligned} p' &= (1+\alpha)(D_{00}+\mathbf{t}^T\mathbf{n})+(1-\alpha)(\mathbf{s}^T\mathbf{m}+\mathbf{t}^T\tilde{D}\mathbf{s}), \\ q' &= (1+\alpha)(D_{00}-\mathbf{t}^T\mathbf{n})+(1-\alpha)(\mathbf{s}^T\mathbf{m}-\mathbf{t}^T\tilde{D}\mathbf{s}). \end{aligned} \tag{9}$$

By the same reasoning as above, we find that, for any fixed values of $(\mathbf{s},\mathbf{t},\alpha)$, the contrast $\mathcal{C}_D(\theta')$ reaches its maximum for either $\beta=0$ or $\beta=1$.

There are thus only four configurations of $(\alpha,\beta)$ that can lead to the maximal contrast. Let us analyze them.

- Purely polarized illumination / purely polarized imaging ($pp$ configuration): this case corresponds to $(\alpha,\beta)=(0,0)$; the contrast in Eq. (4) can be written as

$$\mathcal{C}_D(\mathbf{s},\mathbf{t})=\frac{\mathrm{SNR}_D}{16}\times[D_{00}+\mathbf{s}^T\mathbf{m}+\mathbf{t}^T(\mathbf{n}+\tilde{D}\mathbf{s})]^2. \tag{10}$$

The optimization of this contrast with respect to $\mathbf{s}$ and $\mathbf{t}$ has already been addressed in Ref [19]. We review it here briefly for completeness. For a given illumination vector $\mathbf{s}$, the analysis vector that maximizes the contrast in Eq. (10) is $\mathbf{t}_m(\mathbf{s})=\mathrm{sign}[D_{00}+\mathbf{s}^T\mathbf{m}](\mathbf{n}+\tilde{D}\mathbf{s})/(\|\mathbf{n}+\tilde{D}\mathbf{s}\|)$, where $\mathrm{sign}(x)=1$ if $x>0$, and $-1$ otherwise. Substituting this value in Eq. (10), we obtain

$$\max_{\mathbf{t}}[\mathcal{C}_D(\mathbf{s},\mathbf{t})]=\frac{\mathrm{SNR}_D}{16}\times[|D_{00}+\mathbf{s}^T\mathbf{m}|+\|\mathbf{n}+\tilde{D}\mathbf{s}\|]^2. \tag{11}$$

The maximal contrast in this configuration is thus:

$$\mathcal{C}^{\max}_{\mathrm{pp},D}=\frac{\mathrm{SNR}_D}{16}\times\max_{\mathbf{s}}[F(\mathbf{s})], \tag{12}$$

with

$$F(\mathbf{s})=[|D_{00}+\mathbf{s}^T\mathbf{m}|+\|\mathbf{n}+\tilde{D}\mathbf{s}\|]^2. \tag{13}$$

This contrast is obtained by illuminating the scene with the polarization state $\mathbf{s}_{\max}=\mathrm{argmax}_s[F(\mathbf{s})]$ and analyzing the scattered light with $\mathbf{t}_{\max}=\mathrm{sign}[D_{00}+\mathbf{s}_{\max}^T\mathbf{m}](\mathbf{n}+\tilde{D}\mathbf{s}_{\max})/(\|\mathbf{n}+\tilde{D}\mathbf{s}_{\max}\|)$.

- Purely polarized illumination / intensity imaging ($pi$ configuration): this case corresponds to $(\alpha,\beta)=(0,1)$, and the contrast in Eq. (4) becomes

$$\mathcal{C}_D(\mathbf{s},\mathbf{t})=\frac{\mathrm{SNR}_D}{4}\times[D_{00}+\mathbf{s}^T\mathbf{m}]^2. \tag{14}$$

Equation (14) is maximized when the illumination state of polarization is $\mathbf{s}_{\max}=\mathrm{sign}(D_{00})\times\mathbf{m}/\|\mathbf{m}\|$. The maximal contrast is obtained by substituting this state of polarization in Eq. (14), and one obtains

$$\mathcal{C}^{\max}_{\mathrm{pi},D}=\frac{\mathrm{SNR}_D}{4}\times[|D_{00}|+\|\mathbf{m}\|]^2. \tag{15}$$

- Unpolarized illumination / purely polarized imaging ($up$ configuration): this corresponds to $(\alpha,\beta)=(1,0)$, and the contrast in Eq. (4) becomes

$$\mathcal{C}_D(\mathbf{s},\mathbf{t})=\frac{\mathrm{SNR}_D}{4}\times[D_{00}+\mathbf{t}^T\mathbf{n}]^2. \tag{16}$$

Equation (16) is maximized when the analysis state of polarization is $\mathbf{t}_{\max}=\mathrm{sign}(D_{00})\times\mathbf{n}/\|\mathbf{n}\|$. The maximal contrast is obtained by substituting this state of polarization in Eq. (16), and one obtains

$$\mathcal{C}^{\max}_{\mathrm{up},D}=\frac{\mathrm{SNR}_D}{4}\times[|D_{00}|+\|\mathbf{n}\|]^2. \tag{17}$$

- Unpolarized illumination / intensity imaging ($ui$ configuration): this case corresponds to $(\alpha,\beta)=(1,1)$, and the contrast in Eq. (4) becomes

$$\mathcal{C}^{\max}_{\mathrm{ui},D}=\mathrm{SNR}_D\times[D_{00}]^2. \tag{18}$$

For a given scene, defined by its Mueller matrices $M_a$ and $M_b$, the maximal achievable contrast is

$$\mathcal{C}^{\max}_{D}=\max\{\mathcal{C}^{\max}_{\mathrm{pp},D},\mathcal{C}^{\max}_{\mathrm{pi},D},\mathcal{C}^{\max}_{\mathrm{up},D},\mathcal{C}^{\max}_{\mathrm{ui},D}\}, \tag{19}$$

and the optimal illumination / analysis states are those for which this maximum is obtained.

These results set the domains of optimality of the different imaging configurations in the target detection scenario that we consider. In particular, we reach the interesting conclusion that it is always preferable to purely polarize the illumination ($\alpha=1$), or not to polarize it at all ($\alpha=0$). There is never interest in partially polarizing it. Similarly, for each type of illumination, there is a "turning point" at which polarization imaging becomes preferable to intensity imaging. Interestingly, this turning point is "sharp," in the sense that there is no interest of having a "partially" polarized PSA; it must be totally depolarized (i.e., intensity imaging), or totally polarized.

As a simple example, let us assume that the matrix $D$ is zero, except the term $D_{00}$. This means that the two regions differ only by their intensity reflectivities with respect to unpolarized illumination and not by their polarimetric properties. In this case, $\mathbf{m}=\mathbf{n}=0$, and $\tilde{D}=0$. Obviously, the $ui$ configuration yields the maximal contrast, equal to $\mathrm{SNR}_D\times D_{00}^2$. This is understandable since in this scenario there is no difference in the polarimetric responses of the two regions and the only relevant information comes from the difference of unpolarized intensity reflectivities. The $pi$ and $up$ configurations are equivalent, and give a contrast equal to $\mathrm{SNR}_D\times D_{00}^2/4$. This lower performance can be physically understood by the fact that in the $pi$ case, the

PSG discards half of the light from the unpolarized source, and in the *up* case, the PSA discards half of the useful light coming from the scene, since it is unpolarized. The *pp* configuration yields an even lower contrast of $\mathrm{SNR}_D \times D_{00}^2/16$ since the two above-mentioned effects are simultaneously present. In Section 4, we will provide further illustration of these results by considering more general cases where a polarimetric contrast is present.

### B. Two Intensity Measurements

In the previous subsection we assumed that polarization analysis of the light scattered by the scene consisted of only one intensity measurement. In particular, only the light projected onto the eigenstate of larger eigenvalue is acquired and the rest of the light is lost when a purely polarizing PSA is used. A more efficient way of using the incoming light is to collect the projections on each of the two eigenstates. This can be done easily if the polarizing device involved in the PSA is a polarizing beam splitter that directs the two projections on the orthogonal eigenstates in two different directions, so that both can be acquired. Signal acquisition can be accomplished using one sensor for each channel, or the system can be designed so that the beam splitter directs the two channels on two different parts of the same sensor [23]. Such a system is represented in Fig. 1(b). The PSA is realized with a polarizing beam splitter preceded by a homogeneous polarization modulator whose function is to transform a purely polarized state of polarization of Stokes vector $\mathbf{T}^{\parallel}$ into one of the eigenstates of the beam splitter, which are generally linear. The two channels can thus be considered as generalized polarizers with respective eigenstates $\mathbf{T}^{\parallel} = (1, \mathbf{t})^T$ and $\mathbf{T}^{\perp} = (1, -\mathbf{t})^T$ and corresponding eigenvalues $\mu_{\parallel}$ and $\mu_{\perp}$. The advantage of this architecture with respect to the system studied in the previous section [Fig. 1(a)] is that no light coming from the scene is lost. This benefit comes at the expense of an increase of the complexity of the system.

The signal measured on each channel is

$$i_p^q = \frac{\mu_q \eta I_0}{4} \times [\mathbf{T}^q]^T M_p(\lambda_{\parallel}\mathbf{S}_{\parallel} + \lambda_{\perp}\mathbf{S}_{\perp}) + n_p^q, \tag{20}$$

with $p \in \{a, b\}$ and $q \in \{\parallel, \perp\}$. The contrast on the two channels is

$$\begin{aligned} \mathcal{C}_{2,D}^{\parallel}(\theta) &= \frac{(i_a^{\parallel} - i_b^{\parallel})^2}{\sigma^2} = \frac{\lambda_{\parallel}^2 \mu_{\parallel}^2 \eta^2 I_0^2}{16\sigma^2}[p'' + q'']^2 \\ \mathcal{C}_{2,D}^{\perp}(\theta) &= \frac{(i_a^{\perp} - i_b^{\perp})^2}{\sigma^2} = \frac{\lambda_{\parallel}^2 \mu_{\perp}^2 \eta^2 I_0^2}{16\sigma^2}[p'' - q'']^2, \end{aligned} \tag{21}$$

with

$$\begin{aligned} p'' &= (1+\alpha)D_{00} + (1-\alpha)\mathbf{s}^T\mathbf{m} \\ q'' &= (1+\alpha)\mathbf{t}^T\mathbf{n} + (1-\alpha)\mathbf{t}^T\tilde{D}\mathbf{s}, \end{aligned} \tag{22}$$

and $\theta = (\mathbf{s}, \lambda_{\parallel}, \alpha, \mathbf{t}, \mu_{\parallel}, \mu_{\perp})$. The additive noise terms $n_p^q$ are assumed statistically independent, which implies that the global contrast is simply the sum of the contrasts observed on the two channels:

$$\mathcal{C}_{2,D}(\theta) = \mathcal{C}_{2,D}^{\parallel}(\theta) + \mathcal{C}_{2,D}^{\perp}(\theta). \tag{23}$$

According to Eq. (21), the contrasts $\mathcal{C}_{2,D}^{\parallel}(\theta)$ and $\mathcal{C}_{2,D}^{\perp}(\theta)$ are maximized for $\mu_{\parallel} = \mu_{\perp} = 1$, that is, for a perfect polarizing beam splitter and for $\lambda_{\parallel} = 1$. With these values, Eq. (23) becomes

$$\mathcal{C}_{2,D}(\theta') = \frac{\mathrm{SNR}_D}{8} \times ([p'']^2 + [q'']^2), \tag{24}$$

where $\theta' = (\mathbf{s}, \alpha, \mathbf{t})$, and $\mathrm{SNR}_D$ is defined in Eq. (5). By reasoning similar to that in the previous section, it is easily shown that, for any fixed value of $\mathbf{s}$ and $\mathbf{t}$, $\mathcal{C}_{2,D}(\theta')$, considered as a function of $\alpha$, is convex. Consequently, it is maximal for either $\alpha = 0$ or $\alpha = 1$, and one has two possible configurations.

- Purely polarized illumination ($p2$ configuration): this corresponds to $\alpha = 0$, and the contrast can be written as

$$\mathcal{C}_{2,D}(\mathbf{s}, \mathbf{t}) = \frac{\mathrm{SNR}_D}{8} \times [|D_{00} + \mathbf{s}^T\mathbf{m}|^2 + |\mathbf{t}^T(\mathbf{n} + \tilde{D}\mathbf{s})|^2]. \tag{25}$$

For a given illumination vector $\mathbf{s}$, the analysis vectors that maximize the contrast are $\mathbf{t}_m(\mathbf{s}) = \pm(\mathbf{n} + \tilde{\mathbf{D}}\mathbf{s})/(\|\mathbf{n} + \tilde{\mathbf{D}}\mathbf{s}\|)$. Substituting one of these vectors in Eq. (25), we obtain

$$\max_{\mathbf{t}}[\mathcal{C}_{2,D}(\mathbf{s}, \mathbf{t})] = \frac{\mathrm{SNR}_D}{8} \times [|D_{00} + \mathbf{s}^T\mathbf{m}|^2 + \|\mathbf{n} + \tilde{D}\mathbf{s}\|^2]. \tag{26}$$

The maximal contrast in this configuration is thus:

$$\mathcal{C}_{p2,D}^{\max} = \frac{\mathrm{SNR}_D}{8} \times \max_{\mathbf{s}}[G(\mathbf{s})], \tag{27}$$

with

$$G(\mathbf{s}) = |D_{00} + \mathbf{s}^T\mathbf{m}|^2 + \|\mathbf{n} + \tilde{D}\mathbf{s}\|^2. \tag{28}$$

This result is obtained by illuminating the scene with the polarization state $\mathbf{s}_{\max} = \mathrm{argmax}[G(\mathbf{s})]$. It has been shown in Ref. [15] that $\mathbf{s}_{\max}$ can be determined by solving a sixth-order polynomial equation. The scattered light is analyzed with $\mathbf{t}_{\max} = \pm(\mathbf{n} + \tilde{D}\mathbf{s}_{\max})/(\|\mathbf{n} + \tilde{D}\mathbf{s}_{\max}\|)$.

- Unpolarized illumination ($u2$ configuration): this corresponds to $\alpha = 1$, and the contrast can be written as

$$\mathcal{C}_{2,D}(\mathbf{t}) = \frac{\mathrm{SNR}_D}{2} \times (|D_{00}|^2 + |\mathbf{t}^T\mathbf{n}|^2). \tag{29}$$

This contrast is maximized when the analysis state of polarization is $\mathbf{t}_{\max} = \pm\mathbf{n}/\|\mathbf{n}\|$. The maximal contrast is obtained by substituting this state of polarization in Eq. (29), and one obtains

$$\mathcal{C}_{u2,D}^{\max} = \frac{\mathrm{SNR}_D}{2} \times [|D_{00}|^2 + \|\mathbf{n}\|^2]. \tag{30}$$

It is interesting to compare Eq. (27) with Eq. (12) and to compare Eq. (30) with Eq. (17). It is easily seen that $\mathcal{C}_{p2,D}^{\max} \geq \mathcal{C}_{\mathrm{pp},D}^{\max}$ and $\mathcal{C}_{u2,D}^{\max} \geq \mathcal{C}_{\mathrm{up},D}^{\max}$. In other words, when the PSA is purely polarizing, the contrast is always better with two measurements than with a single one. However, it has to be noticed that the superiority of the two-measurement setup over the one-measurement setup has been established under ideal conditions. In practice, using either two sensors instead of

a single one or using two parts of the same sensor introduces more complexity in the system. For example, the necessary registration of the two images generates errors [23,24]. The level of these drawbacks is implementation-dependent, and in practice, they have to be mitigated with the gain in contrast demonstrated in this section. By considering Eq. (15) or Eq. (18), it is also noticed that intensity-only imaging may yield better contrast than the two-measurement setup.

For example, let us assume again that only $D_{00}$ is nonzero. The contrast obtained with the two-measurement setup under polarized illumination is $\mathrm{SNR}_D \times D_{00}^2/8$. This value is two times larger than that obtained with a single measurement, since the system gathers all the light scattered by the scene thanks to its second channel. For the same reason, the contrast obtained with unpolarized illumination ($\mathrm{SNR}_D \times D_{00}^2/2$) is also two times larger than that obtained with a single measurement. This contrast value is itself smaller than that obtained with unpolarized illumination and intensity imaging ($\mathrm{SNR}_D \times D_{00}^2$). Indeed, the two-measurement setup utilizes two sensors instead of one, and each of these sensors brings its own noise. Consequently, the global noise variance is increased by a factor of 2, and the contrast is reduced by the same factor.

## 3. OPTIMIZATION OF THE CONTRAST IN THE PRESENCE OF BACKGROUND NOISE

In this section, we consider the same imaging architectures as in the previous section but a different model for the noise that perturbs the acquisition. Here we assume that the dominant source of noise is due to the background light that enters the imaging system and is not due to the scattering of active illumination. For example, this passive contribution can be due to scattering of ambient illumination or to emission in the scene. For simplicity's sake we assume that this background illumination is totally unpolarized of average intensity $I_n$. We will call the shot noise due to this passive contribution *background noise*. This noise is additive and can still be considered Gaussian if the number of photons is large (which is the case in most applications). We will see that, in the presence of such noise, the ranking among the different imaging configurations is somewhat modified.

### A. Single Intensity Measurement

Let us first consider the single intensity measurement setup represented in Fig. 1(a). Since it is shot noise, the variance of the background noise is equal to the average number of photoelectrons arriving on the detector; that is,

$$\sigma^2 = (\eta I_n)/2 \times (\mu_\parallel + \mu_\perp). \tag{31}$$

We note that, contrary to detector noise, the variance of background noise depends on the characteristics of the PSA. Substituting Eq. (31) for $\sigma^2$ in Eq. (4), we obtain

$$\mathcal{C}_B(\theta) = \frac{\mu_\parallel \eta \lambda_\parallel^2 I_0^2}{8 I_n (1+\beta)} [(1+\alpha)(1+\beta) D_{00} + (1-\alpha)(1+\beta)\mathbf{s}^T\mathbf{m} + (1+\alpha)(1-\beta)\mathbf{t}^T\mathbf{n} + (1-\alpha)(1-\beta)\mathbf{t}^T\tilde{D}\mathbf{s}]^2. \tag{32}$$

By the same reasoning as in Section 2, it is easily seen that, to maximize the contrast, one has to set $\lambda_\parallel = \mu_\parallel = 1$. The expression to maximize with respect to the other parameters is thus:

$$\mathcal{C}_B(\theta') = \frac{\mathrm{SNR}_B}{8(1+\beta)} \times [p + \beta q]^2, \tag{33}$$

with

$$\mathrm{SNR}_B = \frac{\eta I_0^2}{I_n}. \tag{34}$$

The variables $p$ and $q$ are defined in Eq. (7). It is easily shown that the function $[p+\beta q]^2/(1+\beta)$ is convex. Consequently, the optimal contrast arises in the same four configurations of $(\alpha, \beta)$ as in the case of detector noise (Section 2). In each of these configurations, it is easily seen that the maximal contrasts are obtained for the same illumination/analysis polarization states as in the case of detector noise. However, the relative values of the optimal contrasts are different.

- Purely polarized illumination / purely polarized imaging (*pp* configuration): this corresponds to $(\alpha, \beta) = (0, 0)$, and from Eq. (32); the maximal contrast is

$$\mathcal{C}_{\mathrm{pp},B}^{\max} = \frac{\mathrm{SNR}_B}{8} \times \max_{\mathbf{s}}[F(\mathbf{s})], \tag{35}$$

where $F(\mathbf{s})$ is defined in Eq. (13).

- Purely polarized illumination / intensity imaging (*pi* configuration): this corresponds to $(\alpha, \beta) = (0, 1)$, and from Eq. (32), the maximal contrast is

$$\mathcal{C}_{\mathrm{pi},B}^{\max} = \frac{\mathrm{SNR}_B}{4} \times [|D_{00}| + \|\mathbf{m}\|]^2. \tag{36}$$

- Unpolarized illumination / polarized imaging (*up* configuration): this corresponds to $(\alpha, \beta) = (1, 0)$, and from Eq. (32), the maximal contrast is

$$\mathcal{C}_{\mathrm{up},B}^{\max} = \frac{\mathrm{SNR}_B}{2} \times [|D_{00}| + \|\mathbf{n}\|]^2. \tag{37}$$

- Unpolarized illumination / intensity imaging (*ui* configuration): this corresponds to $(\alpha, \beta) = (1, 1)$, and from Eq. (32), the maximal contrast is

$$\mathcal{C}_{\mathrm{ui},B}^{\max} = \mathrm{SNR}_B \times [D_{00}]^2. \tag{38}$$

We see that, in the presence of background noise, there is again no interest in having a "partially" polarized PSG or PSA. However, the regions of optimality of the four different PSG/PSA configurations are not the same as in the case of detector noise. This is easily understood physically, as the effect arises from the hypothesis that the background light is unpolarized. When this is true, analyzing the incoming light with a purely polarized PSA throws away half of the light and thus divides the background noise variance by two, whereas intensity imaging keeps it entirely. The advantage of intensity imaging thus vanishes sooner than in the presence of detector noise, whose variance is independent of the PSA settings.

As an example, let us assume again that $D$ is zero except $D_{00}$. Under polarized illumination, intensity imaging yields a contrast of $\mathrm{SNR}_B \times D_{00}^2/4$ and polarized imaging a contrast of $\mathrm{SNR}_B \times D_{00}^2/8$. The ratio between the contrast obtained in these two configurations is smaller than in the case of detector noise (2 instead of 4), but intensity imaging still performs twice as well.

### B. Two Intensity Measurements

Let us now consider the two-measurement setup [Fig. 1(b)]. In the presence of background noise, the noise variances on the two channels are $[\sigma_B^{\parallel}]^2 = \lambda_{\parallel}\eta I_n/2$ and $[\sigma_B^{\perp}]^2 = \lambda_{\perp}\eta I_n/2$. The expressions of the contrast are

$$\begin{aligned} \mathcal{C}_{2,B}^{\parallel}(\theta) &= \frac{(i_a^{\parallel} - i_b^{\parallel})^2}{\sigma^2} = \frac{\lambda_{\parallel}^2\mu_{\parallel}\eta^2 I_0^2}{8I_n}[p'' + q'']^2 \\ \mathcal{C}_{2,B}^{\perp}(\theta) &= \frac{(i_a^{\perp} - i_b^{\perp})^2}{\sigma^2} = \frac{\lambda_{\parallel}^2\mu_{\perp}\eta^2 I_0^2}{8I_n}[p'' - q'']^2, \end{aligned} \tag{39}$$

where $p''$ and $q''$ are defined in Eq. (22). Setting $\lambda_{\parallel} = 1$ and $\mu_{\parallel} = \mu_{\perp} = 1$, and by a reasoning similar to that in the previous section, we obtain the following two possible configurations.

- Purely polarized illumination ($p2$ configuration): this corresponds to $\alpha = 0$, and the contrast is

$$\mathcal{C}_{2,B}(\mathbf{s},\mathbf{t}) = \frac{\mathrm{SNR}_B}{4} \times [|D_{00} + \mathbf{s}^T\mathbf{m}|^2 + |\mathbf{t}^T(\mathbf{n} + \tilde{D}\mathbf{s})|^2]. \tag{40}$$

The maximal contrast is thus

$$\mathcal{C}_{p2,B}^{\max} = \frac{\mathrm{SNR}_D}{4} \times \max_{\mathbf{s}}[G(\mathbf{s})], \tag{41}$$

where $G(\mathbf{s})$ is defined in Eq. (28).

- Unpolarized illumination ($u2$ configuration): this corresponds to $\alpha = 1$, and the maximal contrast is

$$\mathcal{C}_{u2,D}^{\max} = \mathrm{SNR}_B \times [|D_{00}|^2 + \|\mathbf{n}\|^2]. \tag{42}$$

By comparing Eq. (41) with Eq. (35) and (36), it appears that $\mathcal{C}_{p2,B}^{\max}$ is always larger than $\mathcal{C}_{\mathrm{pp},B}^{\max}$ and $\mathcal{C}_{\mathrm{pi},B}^{\max}$. Similarly, by comparing Eq. (42) with Eq. (37) and (38), one observes that $\mathcal{C}_{u2,B}^{\max}$ is larger than $\mathcal{C}_{\mathrm{up},B}^{\max}$ and $\mathcal{C}_{\mathrm{ui},B}^{\max}$. In other words, for a given type of illumination (polarized or unpolarized), the two-measurement setup always yields larger contrast than either a polarized single measurement or intensity-only imaging. As an example, let us assume again that $D$ is zero except $D_{00}$. Under polarized illumination, the contrast obtained with two measurements is $\mathrm{SNR}_B \times D_{00}^2/4$ and is thus equal to that obtained with intensity imaging. Under unpolarized illumination, the contrast obtained with two measurements is $\mathrm{SNR}_B \times D_{00}^2$ and is thus again equal to that obtained with intensity imaging.

## 4. DISCUSSION

The main result obtained it the previous sections is that the optimal imaging setup depends on the characteristics of the scene and of the type of noise that affects the measurements. As a summary, Table 1 gives the maximal achievable contrast for each of the different configurations in the presence of detector and background noise sources. These contrast values depend on the difference of the Mueller matrices $D = M^a - M^b$ through the functions $F(\mathbf{s})$ and $G(\mathbf{s})$ defined as

$$F(\mathbf{s}) = (|D_{00} + \mathbf{m}^T\mathbf{s}| + \|\mathbf{n} + \tilde{D}\mathbf{s}\|)^2, \tag{43}$$

$$G(\mathbf{s}) = |D_{00} + \mathbf{m}^T\mathbf{s}|^2 + \|\mathbf{n} + \tilde{D}\mathbf{s}\|^2. \tag{44}$$

**Table 1. Summary of the Maximal Achievable Contrast for Different Acquisition Setups and Different Types of Noise for the Case of the Unpolarized Light Source**

| Configuration | | Detector Noise ($\mathrm{SNR}_D\times$) | Background Noise ($\mathrm{SNR}_B\times$) |
|---|---|---|---|
| One measurement | $pp$ | $\frac{1}{16}\times\max_{\mathbf{s}}[F(\mathbf{s})]$ | $\frac{1}{8}\times\max_{\mathbf{s}}[F(\mathbf{s})]$ |
| | $pi$ | $\frac{1}{4}\times(\lvert D_{00}\rvert + \lVert\mathbf{m}\rVert)^2$ | $\frac{1}{4}\times(\lvert D_{00}\rvert + \lVert\mathbf{m}\rVert)^2$ |
| | $up$ | $\frac{1}{4}\times(\lvert D_{00}\rvert + \lVert\mathbf{n}\rVert)^2$ | $\frac{1}{2}\times(\lvert D_{00}\rvert + \lVert\mathbf{n}\rVert)^2$ |
| | $ui$ | $D_{00}^2$ | $D_{00}^2$ |
| Two measurements | $p2$ | $\frac{1}{8}\times\max_{\mathbf{s}}[G(\mathbf{s})]$ | $\frac{1}{4}\times\max_{\mathbf{s}}[G(\mathbf{s})]$ |
| | $u2$ | $\frac{1}{2}\times(\lvert D_{00}\rvert^2 + \lVert\mathbf{n}\rVert^2)$ | $\lvert D_{00}\rvert^2 + \lVert\mathbf{n}\rVert^2$ |

Up to now, we have assumed that the light source was unpolarized. In some important practical cases, such as illumination with a laser, the light source is intrinsically polarized. In this case, there is no loss of energy induced by polarizing the light source. If the PSG has no loss ($\mu_{\parallel} = 1$), then the intensity of the light emerging from the PSG is multiplied by a factor of 2 compared to the results obtained with unpolarized light source, and thus the contrasts are multiplied by a factor of 4. For the sake of completeness, we have summarized in Table 2 the maximal contrasts obtained with a polarized source when using polarized PSA (configuration $p$), intensity imaging (configuration $i$) and the two-measurement setup (configuration $p2$).

In the remainder of this section, we give some examples of how these results can be used to choose the appropriate polarimetric imaging setup in a given application. Let us first consider the particular case where the target and the background are purely depolarizing, which means that $M^a$ and $M^b$ are diagonal. In this case, $\mathbf{m} = \mathbf{n} = \mathbf{0}$ and $\tilde{D} = \mathrm{diag}(\tilde{d}_1, \tilde{d}_2, \tilde{d}_3)$ is diagonal. Consequently, $F(\mathbf{s}) = (|D_{00}| + \|\tilde{D}\mathbf{s}\|)^2$ and $G(\mathbf{s}) = D_{00}^2 + \|\tilde{D}\mathbf{s}\|^2$. We have $\max_{\mathbf{s}}[F(\mathbf{s})] = (|D_{00}| + \tilde{d}_{\max})^2$ and $\max_{\mathbf{s}}[G(\mathbf{s})] = D_{00}^2 + \tilde{d}_{\max}^2$ with $\tilde{d}_{\max} = \max_i[|\tilde{d}_i|]$. Using these expressions and considering the case of detector noise, it is easily seen from Table 1 that configuration $pp$ will become better than standard imaging (configuration $ui$) when $\tilde{d}_{\max} > 3|D_{00}|$, and configuration $p2$ will become better than configuration $ui$ when $\tilde{d}_{\max} > \sqrt{7}|D_{00}|$. These results are illustrated in Fig. 2, where we have considered that $M^b = \mathrm{diag}(1, 0.3, 0.3, 0.3)$ and $M^a = \mathrm{diag}(0.95, \beta, \beta, 0.3)$, with the parameter $\beta$ varying between 0.1 and 0.5, so that $D_{00} = -0.05$ and $\tilde{d}_{\max} = |\beta - 0.3|$. Figure 2(a) represents the variation of the maximal contrast in the six configurations considered in Table 1 as a function of the parameter $\beta$ in the presence of detector noise. We verify that $\mathcal{C}_{\mathrm{pp},D}^{\max}$ is larger than $\mathcal{C}_{\mathrm{ui},D}^{\max}$ when $\beta < 0.15$ and $\beta > 0.45$, whereas $\mathcal{C}_{p2,D}^{\max}$ is larger than $\mathcal{C}_{\mathrm{ui},D}^{\max}$ when $\beta < 0.17$ and $\beta > 0.43$. We also note that $\mathcal{C}_{p2,D}^{\max}$ is always larger

**Table 2. Summary of the Maximal Achievable Contrast for Different Acquisition Setups and Different Types of Noise for the Case of the Polarized Light Source**

| Configuration | | Detector Noise ($\mathrm{SNR}_D\times$) | Background Noise ($\mathrm{SNR}_B\times$) |
|---|---|---|---|
| One measurement | $p$ | $\frac{1}{4}\times\max_{\mathbf{s}}[F(\mathbf{s})]$ | $\frac{1}{2}\times\max_{\mathbf{s}}[F(\mathbf{s})]$ |
| | $i$ | $(\lvert D_{00}\rvert + \lVert\mathbf{m}\rVert)^2$ | $(\lvert D_{00}\rvert + \lVert\mathbf{m}\rVert)^2$ |
| Two measurements | $p2$ | $\frac{1}{2}\times\max_{\mathbf{s}}[G(\mathbf{s})]$ | $\max_{\mathbf{s}}[G(\mathbf{s})]$ |

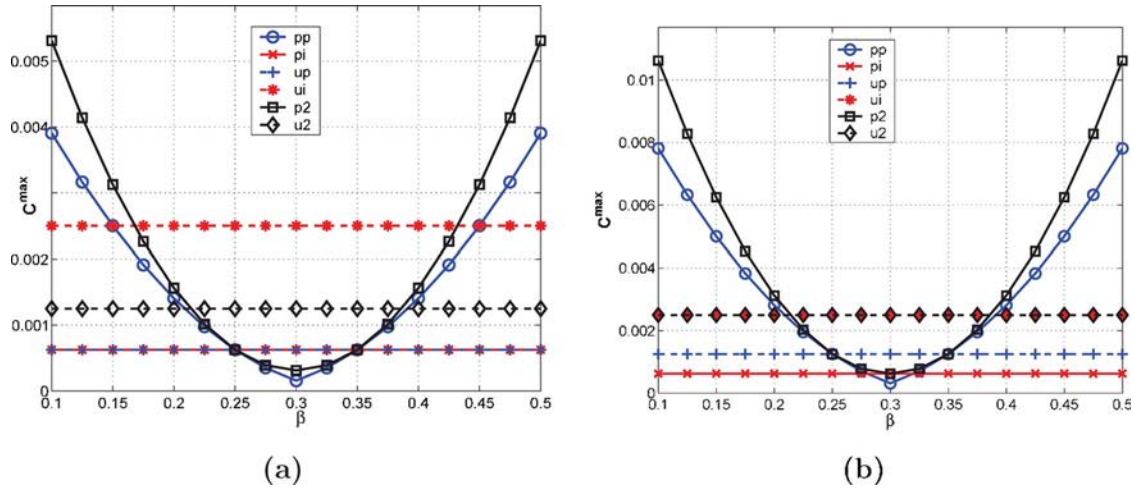


Fig. 2. (Color online) Variation of the maximal achievable contrast as a function of $\beta$ when $M^b = \mathrm{diag}(1, 0.3, 0.3, 0.3)$ and $M^a = \mathrm{diag}(0.95, \beta, \beta, 0.3)$, for the six configurations considered in Table 1 (a) in the presence of detector noise ($\mathrm{SNR}_D = 1$), (b) in the presence of background noise ($\mathrm{SNR}_B = 1$).

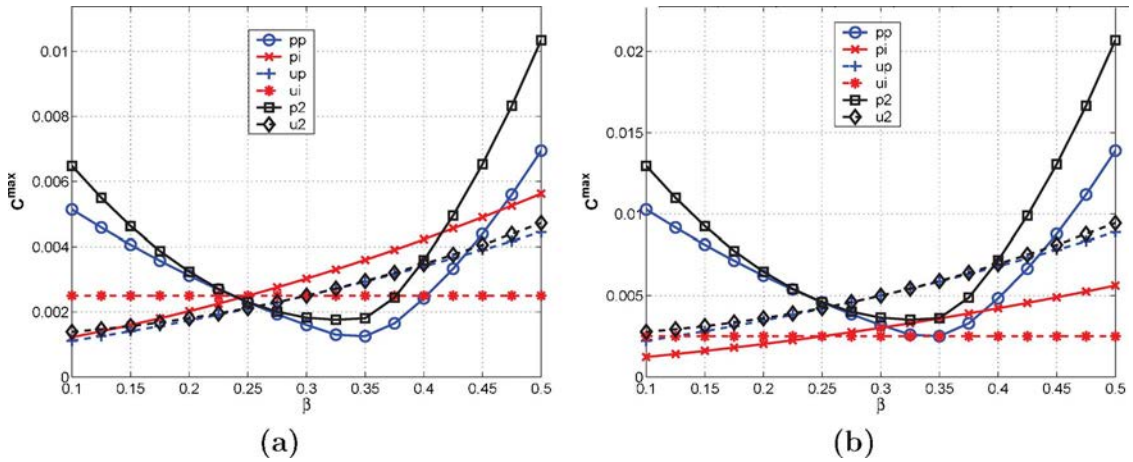


Fig. 3. (Color online) Variation of the maximal achievable contrast as a function of $\beta$ when $M^b = \mathrm{diag}(1, 0.3, 0.3, 0.3)$ and $M^a$ is defined in Eq. (45), for the six configurations considered in Table 1(a) in the presence of detector noise ($\mathrm{SNR}_D = 1$), (b) in the presence of background noise ($\mathrm{SNR}_B = 1$).

than $\mathcal{C}^{\max}_{\mathrm{pp},D}$, and that $\mathcal{C}^{\max}_{\mathrm{pi},D}$ and $\mathcal{C}^{\max}_{\mathrm{up},D}$ are equal and independent of $\beta$ (since $\mathbf{m} = \mathbf{n} = 0$).

In the presence of background noise, it is easily seen from Table 1 that the $pp$ configuration yields better contrast than the $ui$ configuration as soon as $\tilde{d}_{\max} > (\sqrt{8} - 1)|D_{00}|$, and the $p2$ configuration yields better contrast than the $ui$ configuration as soon as $\tilde{d}_{\max} > \sqrt{3}|D_{00}|$. Figure 2(b) represents the variation of the different contrasts as a function of the parameter $\beta$ in the presence of background noise. It can be observed that the curves have exactly the same shapes as in Fig. 2(a) but with different relative levels. This is easily understood by looking at Table 1, where it is seen that, for a given configuration, there is a proportionality factor between the contrasts obtained in the presence of detector and background noises.

Let us take a second example where $M^b$ is the same as it was previously and

$$M^a = \begin{bmatrix} 0.95 & \beta/5 & 0 & 0 \\ \beta/6 & \beta & 0 & 0 \\ 0 & 0 & \beta & 0 \\ 0 & 0 & 0 & 0.3 \end{bmatrix}. \tag{45}$$

This is a fairly general example of a material that has both depolarization and polarizance/diattenuation properties. The target has a diattenuation vector $\mathbf{m} = \beta/5 \times (1, 0, 0)^T$ and a polarizance vector $\mathbf{n} = \beta/6 \times (1, 0, 0)^T$. Figure 3(a) represents the variation of the maximal contrast in the different configurations as a function of $\beta$ in the presence of detector noise. We see that $\mathcal{C}^{\max}_{\mathrm{pi},D}$, $\mathcal{C}^{\max}_{\mathrm{up},D}$, and $\mathcal{C}^{\max}_{u2,D}$ now increase with $\beta$, which is understandable since the norms of $\mathbf{m}$ and $\mathbf{n}$ are proportional to $\beta$. On the other hand, the contrast obtained in configurations that combine polarized illumination and polarized imaging ($\mathcal{C}^{\max}_{\mathrm{pp},D}$ and $\mathcal{C}^{\max}_{p2,D}$) are minimal for values of $\beta$ close to 0.3, since this is the region where the matrix $\tilde{D}$ is smaller, and become larger than the other configurations when $\beta$ is sufficiently large. In the presence of background noise, the behavior is globally the same, but it is noticed that the range of values of $\beta$ for which the polarimetric imaging configurations ($pp$, $up$, $p2$, and $u2$) yield higher contrast than intensity imaging ($pi$ and $ui$) is much increased.

## 5. CONCLUSION

Considering a simple but precisely defined target detection task, we have been able to give a quantitative answer to

the question asked in the title: "when is polarimetric imaging better than intensity imaging?" We have shown that it is never beneficial to use partially polarized illumination or analysis. In other words, the optimal illumination is either unpolarized or purely polarized, and the optimal analysis setup is either unpolarized, which amounts to intensity imaging, or purely polarized. The domains of optimality of these different configurations depend on the Mueller matrices of the target and of the background, on the configuration of the imaging setup, and on the dominant type of noise that perturbs the acquisition. For example, in the case of background noise, we have shown that the two-measurement setup always performs better than intensity imaging for a given type of illumination.

These results give important information to assess the interest of polarimetric imaging in a given application. Of course, they have to be further developed. Interesting topics for future work are to consider more complex scenes and other types of fluctuations, such as signal-dependent photon noise and target variability. Moreover, it is necessary to develop strategies to deal with the case, frequent in practice, when the Mueller matrices of the target and of the background are unknown. We hope to have defined in this paper useful guidelines and methodology for these future works.

## REFERENCES


1. L. B. Wolff, "Polarization vision: a new sensory approach to image understanding," Image Vis. Comput. **15**, 81–93 (1997).
2. J. S. Tyo, D. L. Goldstein, D. B. Chenault, and J. A. Shaw, "Review of passive imaging polarimetry for remote sensing applications," Appl. Opt. **45**, 5453–5469 (2006).
3. M. Alouini, F. Goudail, A. Grisard, J. Bourderionnet, D. Dolfi, I. Baarstad, T. Løke, P. Kaspersen, and X. Normandin, "Active polarimetric and multispectral laboratory demonstrator: contrast enhancement for target detection," Proc. SPIE **6396**, 63960B (2006).
4. P. Terrier, V. Devlaminck, and J. M. Charbois, "Segmentation of rough surfaces using a polarization imaging system," J. Opt. Soc. Am. A **25**, 423–430 (2008).
5. P. J. Wu, J. Joseph, and T. Walsh, "Stokes polarimetry imaging of rat tail tissue in a turbid medium: degree of linear polarization image maps using incident linearly polarized light," J Biomed. Opt. **11**, 014031 (2006).
6. J. M. Bueno, J. Hunter, C. Cookson, M. Kisilak, and M. Campbell, "Improved scanning laser fundus imaging using polarimetry," J. Opt. Soc. Am. A **24**, 1337–1348 (2007).
7. O. Morel, C. Stolz, F. Meriaudeau, and P. Gorria, "Active lighting applied to three-dimensional reconstruction of specular metallic surfaces by polarization imaging," Appl. Opt. **45**, 4062–4068 (2006).
8. A. Ambirajan and D. C. Look, "Optimium angles for a polarimeter: part I," Opt. Eng. **34**, 1651–1658 (1995).
9. D. S. Sabatke, M. R. Descour, E. L. Dereniak, W. C. Sweatt, S. A. Kemme, and G. S. Phipps, "Optimization of retardance for a complete Stokes polarimeter," Opt. Lett. **25**, 802–804 (2000).
10. J. S. Tyo, "Noise equalization in Stokes parameter images obtained by use of variable-retardance polarimeters," Opt. Lett. **25**, 1198–1200 (2000).
11. J. S. Tyo, "Design of optimal polarimeters: maximization of the signal-to-noise ratio and minimization of systematic error," Appl. Opt. **41**, 619–630 (2002).
12. S. N. Savenkov, "Optimization and structuring of the instrument matrix for polarimetric measurements," Opt. Eng. **41**, 965–972 (2002).
13. A. A. Swartz, H. A. Yueh, J. A. Kong, L. M. Novak, and R. T. Shin, "Optimal polarizations for achieving maximal contrast in radar images," J. Geophys. Res. **93**, 15252–15260 (1988).
14. M. Floc'h, G. Le Brun, C. Kieleck, J. Cariou, and J. Lotrian, "Polarimetric considerations to optimize lidar detection of immersed targets," Pure Appl. Opt. **7**, 1327–1340 (1998).
15. F. Goudail, "Optimization of the contrast in active Stokes images," Opt. Lett. **34**, 121–123 (2009).
16. J. S. Tyo, S. J. Johnson, Z. Wang, and B. G. Hoover, "Designing partial Mueller matrix polarimeters," Proc. SPIE **7461**, 74610V (2009).
17. A. B. Kostinski and W. M. Boerner, "On the polarimetric contrast optimization," IEEE Trans. Antennas Propag. **35**, 988–991 (1987).
18. F. Goudail and A. Bénière, "Optimization of the contrast in polarimetric scalar images," Opt. Lett. **34**, 1471–1473 (2009).
19. F. Goudail, "Comparison of the maximal achievable contrast in scalar, Stokes and Mueller images," Opt. Lett. **35**, 2600–2602 (2010).
20. D. Goldstein, *Polarized Light*, 2nd ed. (Marcel Dekker, 2003).
21. P. Réfrégier and F. Goudail, "Invariant polarimetric contrast parameters for coherent light," J. Opt. Soc. Am. A **19**, 1223–1233 (2002).
22. F. Goudail, P. Réfrégier, and G. Delyon, "Bhattacharyya distance as a contrast parameter for statistical processing of noisy optical images," J. Opt. Soc. Am. A **21**, 1231–1240 (2004).
23. A. Bénière, F. Goudail, M. Alouini, and D. Dolfi, "Design and experimental validation of a snapshot polarization contrast imager," Appl. Opt. **48**, 5764–5773 (2009).
24. M. H. Smith, J. B. Woodruff, and J. D. Howe, "Beam wander considerations in imaging polarimetry," Proc. SPIE **3754**, 50–54 (1999).